

Fabrication of Zr-based Metal Organic Framework and Its Application in to Photocatalysis and Electrocatalysis by Dye Removal Studies

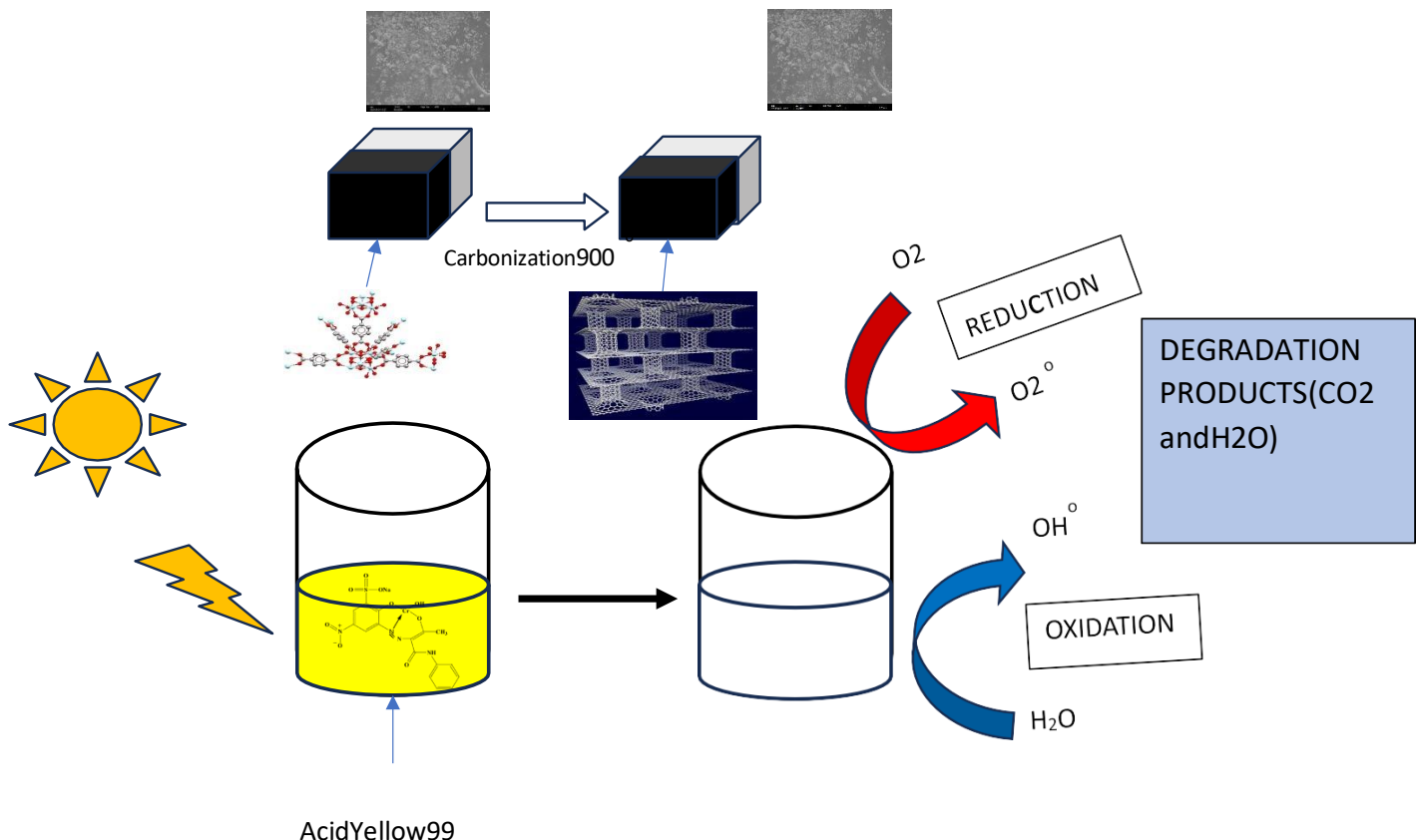
Mr. Harishkumar Sivaraju
Research Scholar, UG and Research Department of Chemistry, Erode Arts and Science College (Autonomous),
Erode – 638 009 Tamil Nadu, India
(Affiliated to Bharathiar University, Coimbatore-641046)

Dr. Santhi Mariappan
Associate Professor and Head, UG and Research Department of Chemistry, Erode arts and Science College (Autonomous), Erode – 638 009 Tamil Nadu, India (Affiliated to Bharathiar University, Coimbatore - 641 046)

Abstract - In this work, the photocatalytic degradation of Acid Yellow, 99 (AY 99) dye under solar light irradiation using the Zr-MOF@GNS and synthesized ZrO₂ is investigated. The ZrO₂ is synthesized using Zr-metal precursor. The prepared ZrO₂ is used to synthesize Zr-MOF@GNS and it is further examined using FT-IR, PXRD and FESEM analyses. The photocatalytic degradation of AY99 is studied by varying the initial concentration of AY99, the length of the irradiation period, the catalyst dose and the pH of the dye solution. From the result it is found that the Zr-MOF@GNS is an efficient and promising catalyst for the enhancement of photocatalytic degradation of AY99. Electrochemical studies show that ZrO₂ and Zr-MOF@GNS can act as electrocatalyst for acid base titrations.

Keywords : ZrO₂ Zr-MOF@GNS, AY99, Photocatalysis and Electrocatalysis,.

Graphical abstract



INTRODUCTION:

The toxicity and environmental persistence of MB poses serious risks: "One of the popular acidic dyes that is environmentally persistent, toxic, carcinogenic and mutagenic is Acid Yellow 99[01]. Health effects range from respiratory distress, tissue necrosis, and jaundice to oxidative damage, due to MB's monoamine oxidase inhibition and its water solubility. MB also enters food chains, impairing aquatic life and posing bioaccumulation risks [02]

Acid Yellow 99 (AY-99) is an azo dye commonly used in the textile and leather industries for its vibrant yellow color. The chemical structure of AY-99, which includes an azo bond (-N=N-) and aromatic rings, makes it highly resistant to biodegradation and other conventional removal methods. The persistence of such dyes in aquatic environments poses significant ecological and health risks. AY-99, like many azo dyes, is toxic to aquatic organisms and can disrupt ecosystems by decreasing oxygen levels in water bodies [3]. The coagulation process effectively decolorizes insoluble dyes, but it fails to work well with soluble dyes. Traditional methods for removing dyes from wastewater include adsorption, chemical oxidation, biological treatment and membrane filtration [4]. However, these techniques often come with limitations such as incomplete dye removal, generation of secondary pollutants, or high operational costs. They are effective but tend to be energy-intensive and may generate toxic by-products [5]. Biological treatments, while environmentally friendly, may not be effective for recalcitrant dyes like AY-99 due to their complex molecular structure and resistance to microbial degradation. The long-term presence or accumulation of these dyes in waste water discharged from these industries is detrimental to the aquatic environment. Given these challenges, the need for more efficient, sustainable, and eco-friendly methods to degrade organic pollutants, including dyes, is crucial [6]. Synthetic dyes are widely used in various industries such as textiles, leather, paper, plastics, and cosmetics, leading to the discharge of large volumes of dye-containing effluents into water bodies. These dyes, particularly **methylene blue**,

crystal violet, and **rhodamine B**,**Acid yellow 99** are not only toxic and carcinogenic but also resistant to biological degradation due to their complex aromatic molecular structures. Hence, effective and eco- friendly strategies for dye removal are essential for environmental protection.

Among several advanced oxidation processes, **photocatalytic degradation** has emerged as a highly promising method for dye removal due to its **cost-effectiveness, reusability, and ability to completely mineralize yes under light irradiation.**

This process typically utilizes **semiconductor photocatalysts** (e.g., TiO₂, ZrO, g- C₃N₄) that, under UV or visible light, generate electron-hole pairs capable of producing reactive oxygen species (ROS) such as hydroxyl radicals (•OH) and superoxide radicals (•O₂⁻), which attack and break down dye molecules into non- toxic end products like CO₂ and H₂O.

Key Features and Efficiency of Photocatalytic Degradation

- **Eco-friendly and non-selective:** Can degrade a wide range of organic pollutants without the need for additional chemicals.
- **Low energy requirement:** Especially under visible light or sunlight, making it suitable for sustainable applications.
- **No secondary pollution:** Unlike adsorption or chemical treatments, photocatalysis does not produce harmful residues.
- **Regenerability:** Photocatalysts can be reused multiple times with minimal loss in activity [7].

Recent studies have shown enhanced performance through **doping, composite formation, and nanostructuring** of photocatalysts. For instance, **Ag-doped ZnO nanocomposites** demonstrated superior visible-light-driven degradation efficiency for methylene blue dye, attributed to better charge separation and light absorption [8].

Photocatalytic degradation offers a viable solution by utilizing light energy to drive chemical reactions that break down harmful pollutants into non-toxic by-products, such as water and carbon dioxide [9]. However, the application of photocatalysis for environmental remediation is still a challenging task.

Metal-organic frameworks (MOFs) are a class of materials consisting of metal ions or clusters coordinated to organic ligands, forming a highly porous, crystalline structure. MOFs have gained significant attention as photocatalysts due to their high surface area, tunable structure, and ability to adsorb a wide variety of organic pollutants [10]. metal-organic framework (MOF) possesses high surface area, chemical tunability, and abundant active adsorption sites, resulting in MOF adsorbents exhibit high adsorption capacity for metal ions. These properties make MOFs ideal candidates for applications in environmental remediation, including photocatalytic degradation of dyes [11, 12]. Among various MOFs, zirconium-based MOFs (Zr-MOFs) have shown exceptional promise due to their high stability, large surface area, and ability to enhance photocatalytic performance.

monoclinic ZrO₂, a key component in Zr-MOFs, is known for its excellent chemical

stability, thermal resistance, and low toxicity. These properties make ZrO₂-based MOFs highly suitable for photocatalytic applications, especially in harsh environments where other photocatalysts might degrade or lose activity. Zr-MOFs are also highly stable in aqueous environments, a critical factor for wastewater treatment processes [13-15].

Metal-Organic Frameworks (MOFs) have emerged as one of the most promising classes of photocatalysts for the degradation of organic dyes from wastewater. Due to their **high surface area, tunable porosity, structural diversity, and photoactive metal centers**, MOFs offer superior photocatalytic performance compared to conventional semiconductors like ZrO. MOFs such as **MIL-125(Ti)**, **UiO-66(Zr)**, and **NH₂-MIL-88B(Fe)** exhibit excellent light absorption and charge separation capabilities, facilitating the generation of reactive oxygen species (ROS) under UV and visible light [16]. Furthermore, the integration of light-harvesting linkers (e.g., amino-terephthalate) into the MOF structure enhances the absorption in the visible region, making them ideal for solar-driven degradation. Additionally, MOFs can be **post-synthetically modified** or composited with other materials like graphene oxide or noble metals to further enhance photocatalytic efficiency and stability [17]. Notably, studies have shown that MOF-based photocatalysts exhibit high degradation efficiency toward common dyes such as **methylene blue**, **rhodamine B**, and **crystal violet**, achieving nearly complete mineralization without generating toxic byproducts. In addition, the crucial electronic and/or surface structures of hollow and/or porous nanostructures can be tuned with the use of MOFs, thereby promoting electrocatalytic activity [18]. The present study focuses on photocatalytic applications of ZrO₂ and Zr-MOF@GNS using AY99 dye as a model compound. The electrochemical studies done using strong acid and

strong base titrations.

2. EXPERIMENTAL

Materials

The AY99 dye is purchased commercially from local vendors ($C_{25}H_{19}N_4NaO_8S_2$, CAS:10343-58-5). De-ionized water used in the process. Zirconium oxychloride is procured from Nice chemicals (P) Ltd. and all other reagents are used as such without further purification.

Synthesis of ZrO_2

ZrO_2 is synthesized by mixing 0.1 M of NaOH with a 2 mM solution of melamine and 2.5 mM of zirconium oxychloride in a magnetic stirrer. The loosely bonded metal residue is baked in a muffle furnace at $900^{\circ}C$ for 12 hours to produce white powder after being repeatedly cleaned by centrifugation with alcohol.

Synthesis of Zr-MOF@GNS

In order to accomplish carbonization, the sample is placed in a microwave oven and heated to around $500^{\circ}C$ for three hours while being exposed to oxygen. To oxidise the ZrO_2 , the sample is allowed to cool to ambient temperature before being annealed for an hour at $300^{\circ}C$ in an air oven.

2.3 Conductometric determination

The conductometric titration of strong acid and strong base is carried out using ZrO_2 and Zr-MOF@GNS as an electrocatalyst. 0.1 N of HCl is titrated with 0.5 N NaOH solution by adding 0.005 g/l of Zr-MOF@GNS. The values observed are plotted against the volume of NaOH added from the curve obtained; the end point is determined graphically.

3. RESULT AND DISCUSSION

Characterization

The synthesized Zr-MOF@GNS and ZrO_2 are examined using FT-IR, FESEM and PXRD analyses. The surface morphology of ZrO_2 and Zr-MOF@GNS is characterized using a scanning electron microscope (SEM, Hitachi S-4800). Fourier Transform Infrared Spectroscopy (FT-IR) measurements are carried out with a SHIMADZU IRTRACER 100, utilizing the KBr pellet method over a range of $4500\text{--}500\text{ cm}^{-1}$. The crystalline phase structure is confirmed via Powder X-ray Diffraction (PXRD) using a BRUKER USA D8 Advance DaVinci diffractometer with Cu-K α radiation, scanning from 0° to 100° . [19-20]

FT-IR Analysis

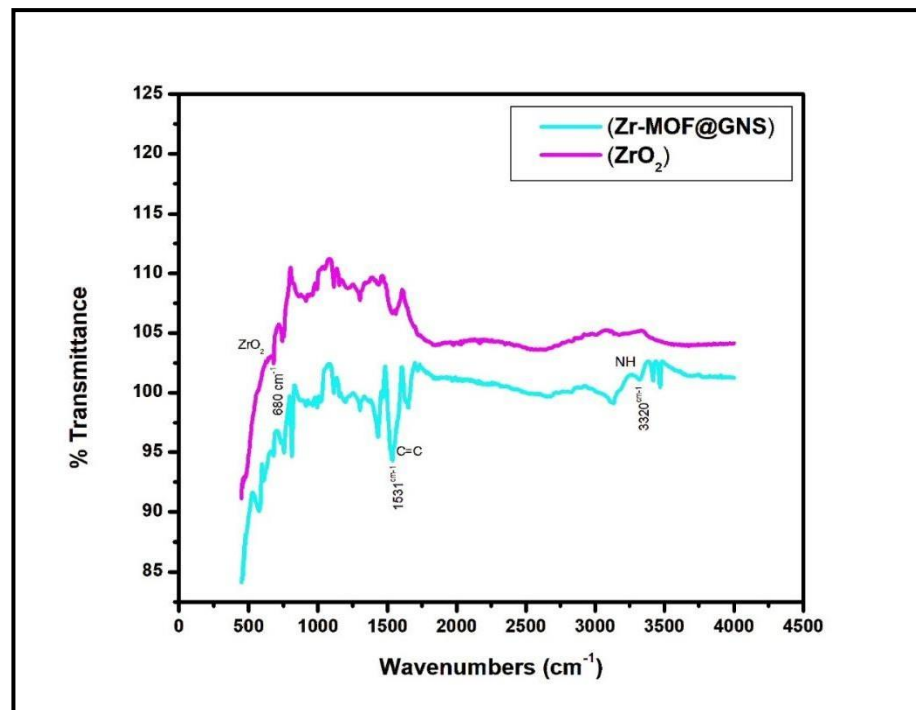


Fig1 FT-IR spectral analysis of Zr-MOF@GNS and ZrO₂

Fourier-Transform Infrared (FTIR) spectroscopy was employed to elucidate the chemical functional groups and confirm the successful synthesis of the Zr-MOF@GNS nanocomposite. The spectra for the pristine ZrO₂ and the Zr-MOF@GNS composite are presented in Fig. 01

The synthesized ZrO₂ nanoparticles exhibited a broad absorption band in the range of 400-700 cm⁻¹, which is characteristic of the stretching vibrations of Zr-O bonds [21]. Additional bands observed at 1630 cm⁻¹ and 3400 cm⁻¹ were assigned to the H-O-H bending and O-H stretching modes of water molecules, respectively, a common feature in metal oxides with high surface area [22].

The incorporation of melamine was evidenced by the distinct N-H stretching vibrations, manifesting as a series of medium-sharp bands in the 3200-3500 cm⁻¹ region [23-24]. Furthermore, the C=C skeletal vibrations from the graphitic sp² carbon domains of the graphenenanocomposite were identified as a shoulder near 1500-1600 cm⁻¹, overlapping with the carboxylate signals. The Zr-O stretching vibrations from the inorganic secondary building units (SBUs) of the MOF contributed to the broad absorption features below 800 cm⁻¹ [25, 26].

The collective evidence from the FTIR analysis confirms the successful formation of the Zr-MOF structure, its functionalization with melamine, and its composite nature with graphenenanocomposite [27].

PXRD Analysis

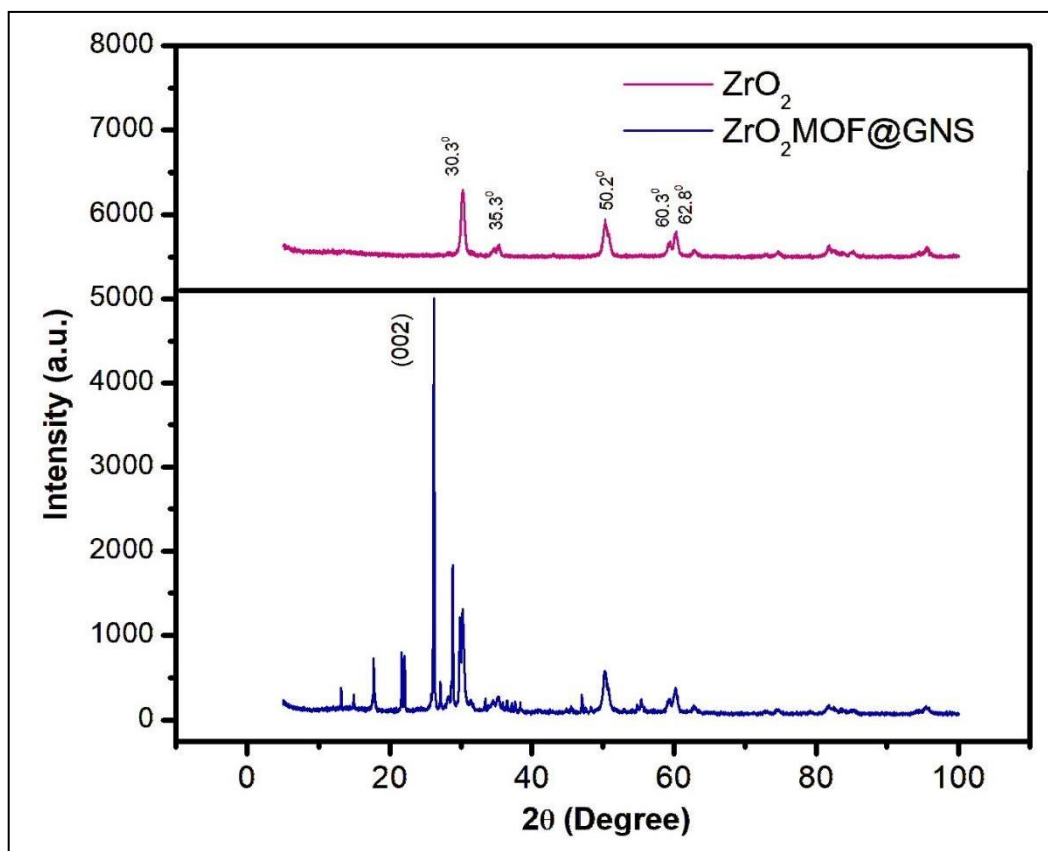


Fig3PXRDanalysisof(a)ZrO₂and(b)Zr-MOF@GNS

Major diffraction peaks appear at $2\theta \approx 30.3^\circ$, 35.3° , 50.2° , 60.3° , and 62.8° , consistent with the tetragonal phase of ZrO₂ (JCPDS49-1642). The presence of sharp, well-defined peaks signals high crystallinity and phase purity, which directly correlates with the photocatalytic activity of ZrO₂-based systems. Such nanoscale, highly crystalline ZrO₂ is acknowledged for efficient charge separation during photocatalytic reactions a factor repeatedly demonstrated as enhancing pollutant degradation rates. Particle size calculation using the Scherrer equation

$$D = 0.9 \lambda / \beta \cos \theta$$

yields an average size around ZrO₂ is 0.1101 nm and Zr-MOF@GNS is 0.1022 nm as a result that closely matches values commonly reported for ZrO₂ nanostructures and GNS product formed. The subtle peak near $2\theta \approx 26.5^\circ$ is attributed to the (002) plane of graphitic carbon, evidencing successful incorporation of graphene nanosheets within the composite. The absence or attenuation of some parent ZrO₂ peaks and the emergence of new or broadened reflections in the composite confirm the formation of the zirconium MOF structure and integration with GNS. Zr-MOF composites regularly highlight MOF-related manifold reflections spanning $2\theta \approx 20$ –30°, further supporting successful framework formation. [28-35]

FESEM Analysis

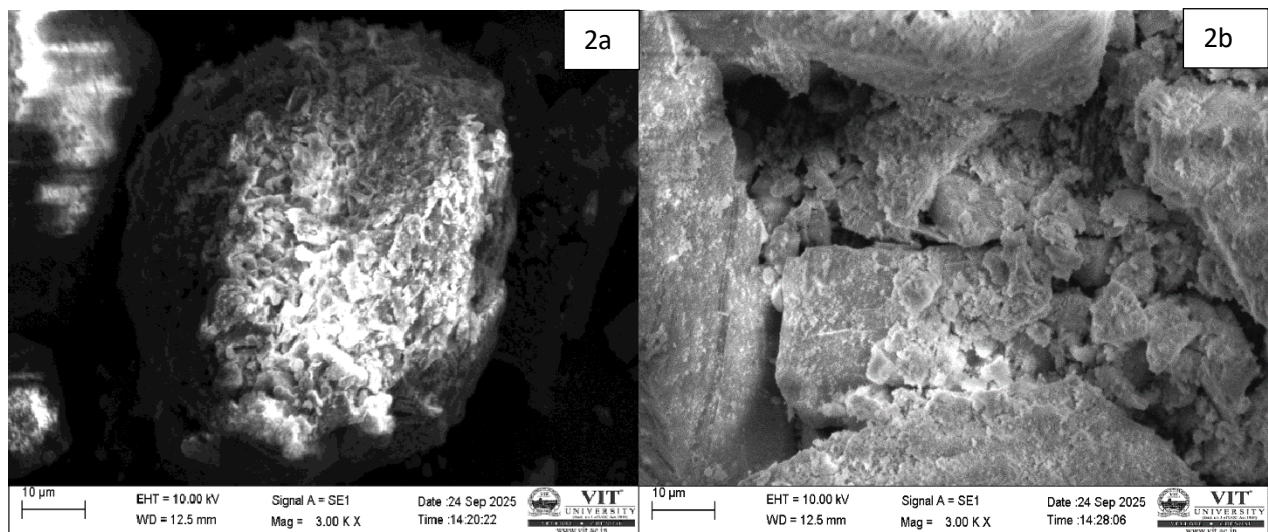


Fig2aand2bZrO₂SEM(2a),Zr-MOFSEM(2b) images

The fig. 2a depicts that the ZrO₂ particles are in amorphous state due to aggregating or overlapping of smaller particles there are some larger particles. The SEM pictures clearly exhibit that the grains are randomly distributed with smaller size and it is

noticed that the particles are of homogeneous spherical shape, and are dusty and messy in with sharp edges in the corners and are slightly crystalline. Above images are information of the shape and structure of the particles synthesized [36]. Fig. 2b evident that the synthesized Zr-MOF@GNS is in crystalline state and are brittle in nature. The improved morphology is advantageous for photocatalytic and electrocatalytic application as it ensures a higher surface area and better accessibility to active sites.

Photocatalytic Application

Effect of initial concentration of AY99 dye

In order to study the effect of initial concentration of solution by the catalysts such as ZrO₂ and Zr-MOF@GNS, the amount of the catalysts dosage is kept constant and different initial concentrations are varied in the particular time interval.

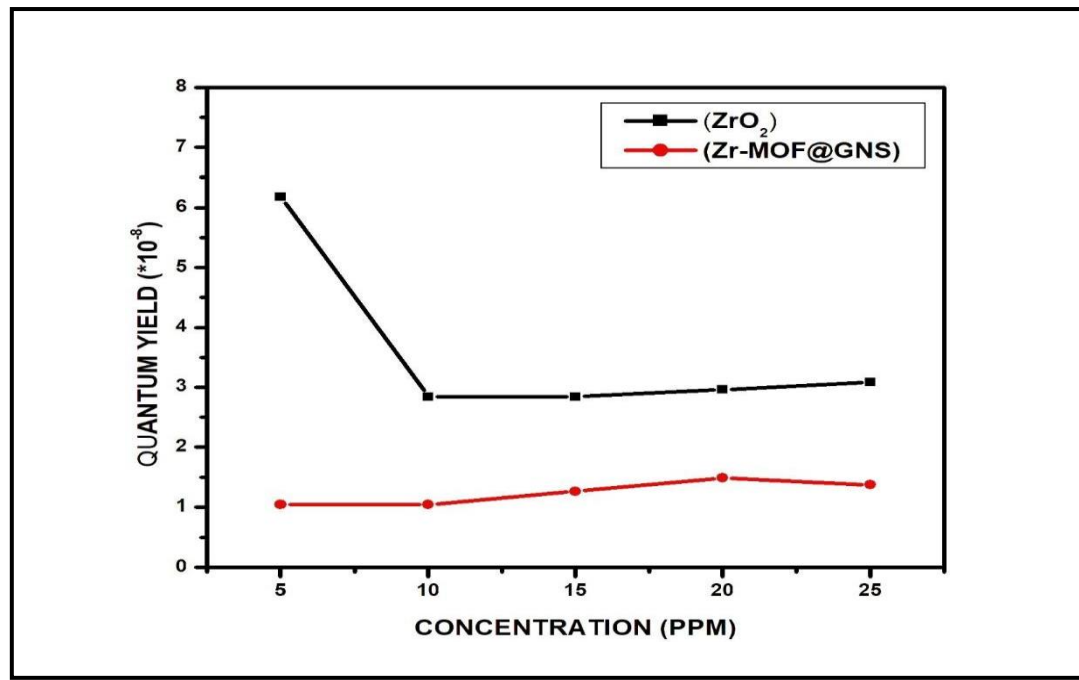


Fig4 - Effect of initial concentration on the photodegradation of AY99 under solar light irradiation

The observed results revealed that the quantum yield of the photocatalysis process increases with increase in initial concentration of AY99 dye. This can be explained in terms of availability of active sites on the catalyst surface and the penetration of solar light into the suspension. The total active surface increases in the AY99 increases with increase in the concentration which tends to increase in the removal [37].

The length of the irradiation period

In order to study the length of irradiation period on the removal of AY99 dye by photocatalytic degradation process on ZrO_2 and Zr-MOF@GNS, the degradation experiments are carried out at constant amount of the catalysts and optimum initial concentration but varying the irradiation period.

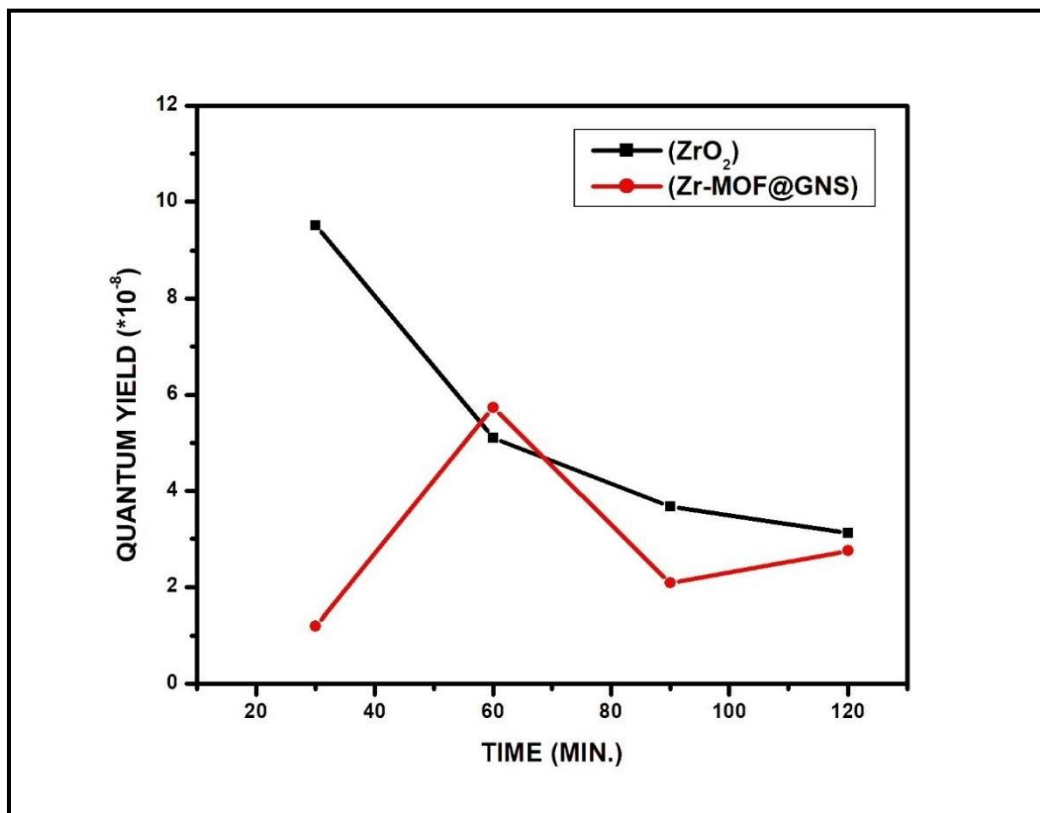


Fig5: The length of the irradiation period of the photodegradation of AY99 under solar light irradiation

The length of irradiation period plays an important role in degradation process of pollutants. The length of irradiation period is varied from 30 to 180 min. The results reveal that the quantum yield of the reaction decreases with increase in irradiation period. It is observed that Zr-MOF@GNS / solar light system exhibits better photocatalytic efficiency than that of ZrO_2 / solar light system. [38]

Thecatalystdose

To study the effect of the catalyst dose, the amount of ZrO_2 and Zr-MOF@GNS is varied, the initial concentration of AY99 dye solution in each case is kept constant at optimum value.

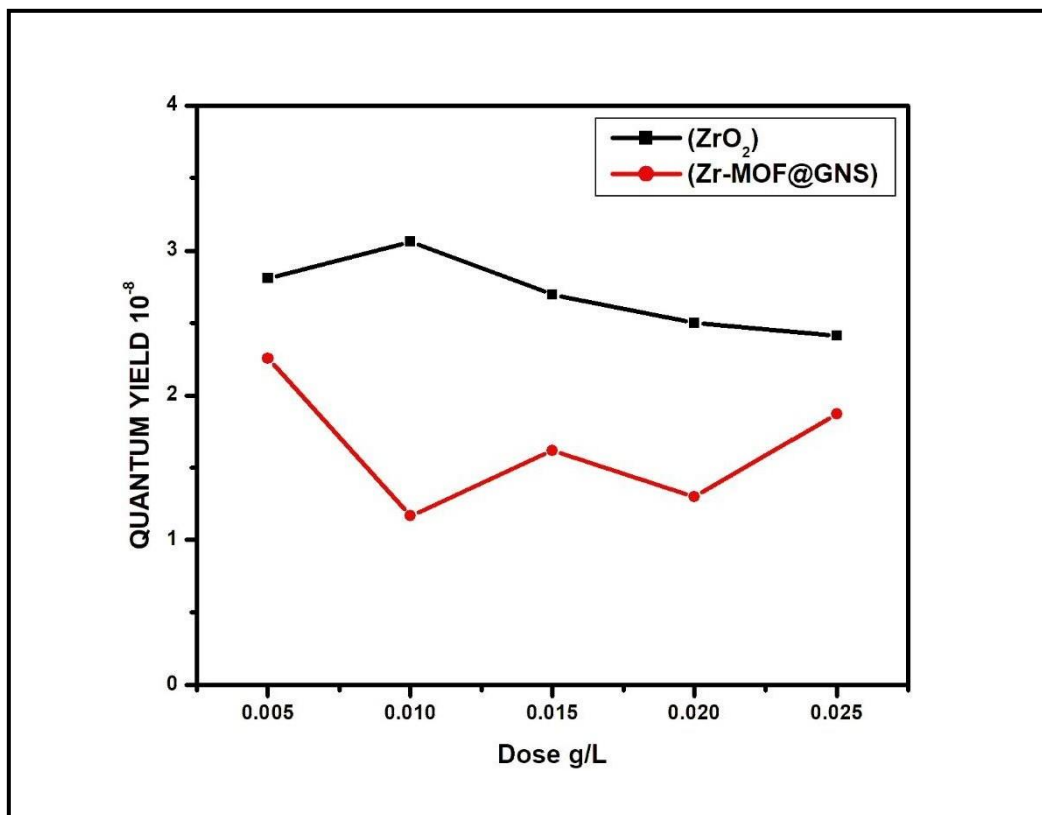


Fig6 - ThecatalystdosevariationofthephotodegradationofAY99undersolarlight irradiation

Optimizing the amount of ZrO_2 and Zr-MOF@GNS is done in order to obtain the maximum amount of quantum yield in the photocatalytic degradation process. Hence in this study the quantity of the catalyst is varied from 0.005 g/L to 0.025 g/L. It is noticed that the quantum yield of the reaction increases with an increase in the amount of ZrO_2 and Zr-MOF@GNS. This is due to the fact that an increase in the catalyst dose the number of active sites on the surface of the catalyst increases and hence the quantum yield of the reaction increases. [39]

ThepHof the dye solution:

The photo degradation experiments are carried out at different initial pH at constant optimum initial concentration of AY99 dye solution, the amount of the catalyst and irradiation time.

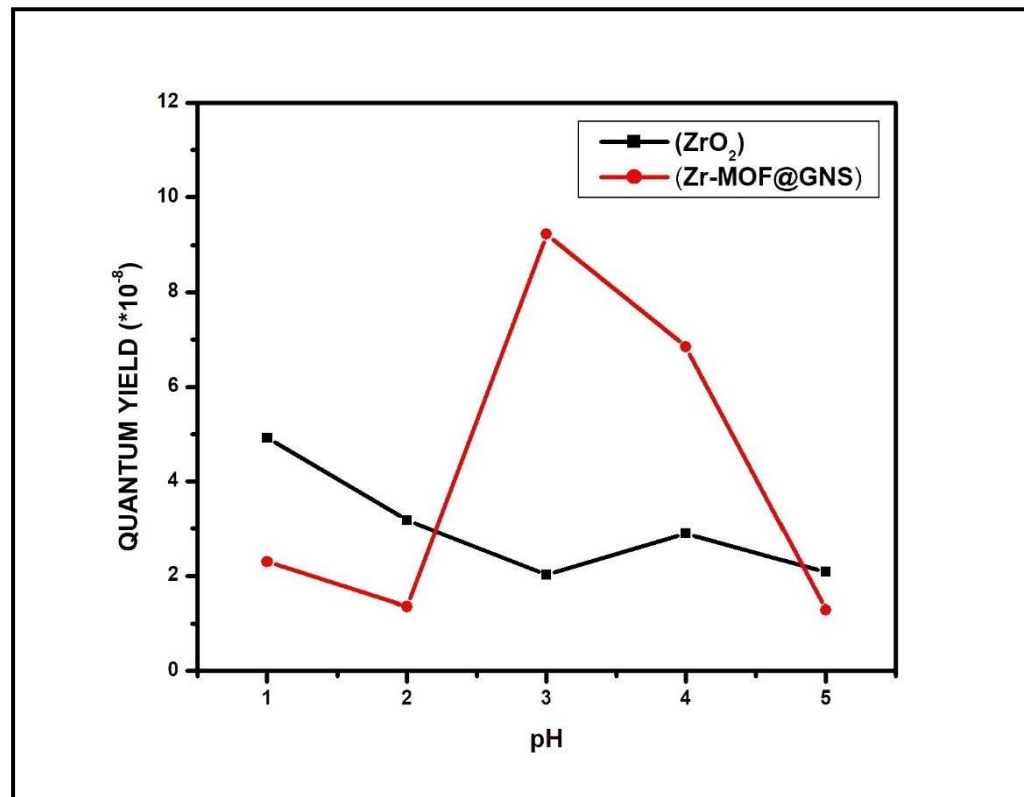


Fig7 - The pH of the dye solution is varied on the photodegradation of AY99 under solar light irradiation

The pH value is one of the important factors influencing the quantum yield of the photodegradation process of pollutants especially dyes. The AY99 dye degradation is highly pH dependent. The photocatalytic degradation of AY99 dye at different pH values varying from 1 to 5, clearly shows that the quantum yield efficiency is higher in acidic medium. The Zr-MOF@GNS having high efficiency for photodegradation of AY99 dye. [40]

4.0 pictorial explanation

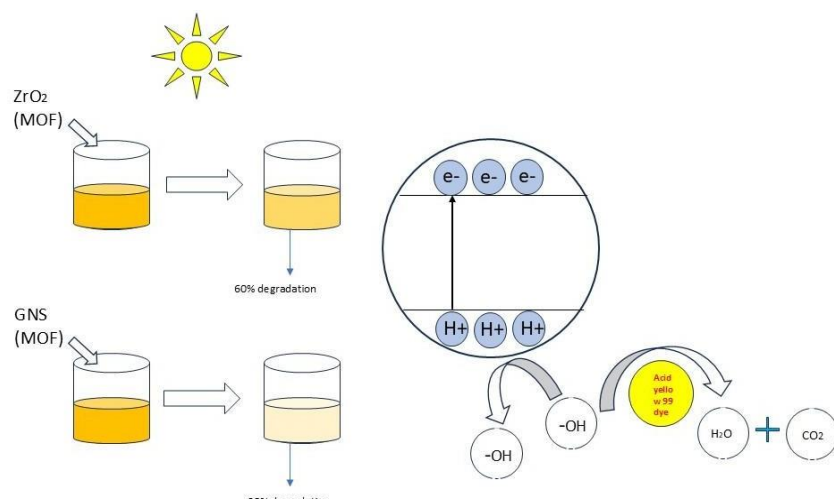


Fig9

4.1 Mechanism of photodegradation of AY99 dye

Using a photocatalyst—usually a semiconductor material like TiO_2 , ZnO or ZrO_2 —to capture solar energy and break down dye molecules is known as photocatalytic degradation of hazardous dyes under sunlight. The photocatalyst creates electron-hole pairs by absorbing photons when exposed to sunshine. Reactive oxygen species (ROS) like hydroxyl radicals ($\cdot OH$) and superoxide anions ($O_2^- \cdot$) are created when excited electrons (e^-) and holes (h^+) engage in redox processes. When the dye molecules are attacked by these very reactive species, they are broken down into smaller, less hazardous, or mineralized chemicals like CO_2 and H_2O . This environmentally friendly technique efficiently eliminates colors from wastewater.

Photons from sunlight with energy equal to or higher than its bandgap are absorbed by zirconium oxide. Positively charged holes (h^+) were left in the valence band after these energised electrons (e^-) in the valence band were promoted to the conduction band.

The electron-hole pairs interact with molecules in the environment. The holes (h^+) can oxidize water (H_2O) or hydroxide ions (OH^-) to generate highly reactive hydroxyl radicals ($\cdot OH$). Simultaneously, the electrons (e^-) reduce oxygen molecules (O_2) to form superoxide anions ($O_2^- \cdot$).



The dye molecules are attacked by the very reactive superoxide anions ($O_2^- \cdot$) and hydroxyl radicals ($\cdot OH$). By cleaving bonds and starting oxidation processes, these radicals split the complex colour molecules into smaller pieces.



The dye eventually mineralizes into non-toxic substances including carbon dioxide (CO_2), water (H_2O) and inorganic ions as a result of the intermediates created during the breakdown process being further oxidized over time. The photocatalyst is not consumed during the reaction, is making the process sustainable. It can continue to catalyze reactions as long as it is exposed to sunlight and is not fouled or degraded. This process is eco-friendly and efficient for treating dye-contaminated wastewater, as it utilizes sunlight (a renewable energy source) and does not produce harmful secondary pollutants. [41]

5.0 APPLICATION TO CONDUCTIVITY:

From the catalyst which are used in the photocatalytic degradation are verified in order to check the conductivity of the synthesized photocatalyst.

5.1 Electrochemical reaction is studied using ZrO_2 and Zr -MOF

Fig depicts the electrochemical acid base titration reaction of $NaOH$ vs HCl using ZrO_2 and Zr -MOF@GNS as an electro catalyst. the observed results indicate that the end point of the reaction decreases significantly while using Zr -MOF@GNS compared to that of ZrO_2 .

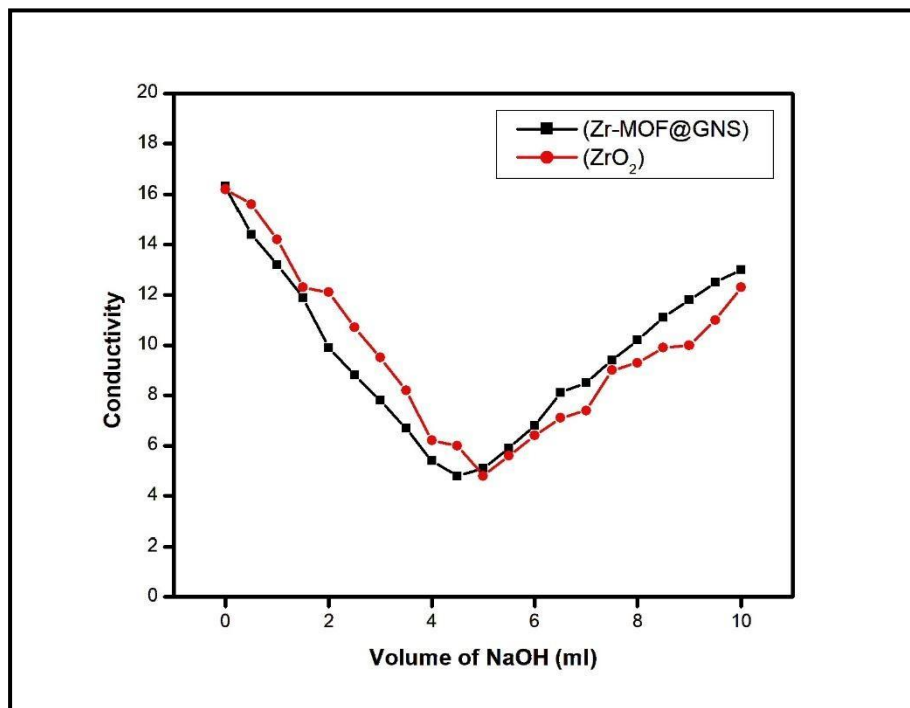


Fig8Electrochemical studies of ZrO_2 and Zr-MOF@GNS

6. CONCLUSION:

The photocatalytic activity of ZrO_2 and Zr-based MOFs studied under sunlight as source for the photodegradation of AY99 dye. The effect of initial concentration, the length of irradiation time, catalyst dose used and pH of the dye solution is studied and the reaction conditions are optimized. The mechanism of photocatalytic degradation takes place through the formation of reactive oxygen species (ROS) such as hydroxyl radicals ($\cdot\text{OH}$) and superoxide anions ($\text{O}_2^{\cdot-}$). The electro chemical studies indicate that Zr-MOF@GNS increase the rate of the reaction. From the results it can be concluded that Zr-MOF@GNS catalyst and ZrO_2 act as photo and electro catalyst.

ACKNOWLEDGEMENT

The authors thanks, The Management and The Principal of Erode Arts and Science College (Autonomous), Erode, – 638009 Tamil Nadu, India for providing the necessary facilities to complete this work.

REFERENCES

- [1] carbon and composites. "ACSSustainableChem.Eng., 2020, 8(1), 109–120.
- [2] Weifeng Zhang, Na Liu, Liangxin Xu, Ruixiang Qu, Yuning Chen, Qingdong Zhang, Yanan Liu, Yen Wei, and Lin Feng "polymer Decorated Filter Material for Wastewater Treatment: In situ Ultrafast Oil/water Emulsion Separation and Azo Dye Adsorption"
- [3] Zhang, L., et al. "Photocatalytic degradation of dyes using TiO_2 -based catalysts." ACS Appl. Mater. Interfaces, 2019, 11(34), 31452-31460.
- [4] Gopalakrishnan, A., et al. "Photocatalytic oxidation of organic pollutants." ACS Catal., 2017, 7(7), 4687-4695.
- [5] Zhang, S., et al. "Fenton-like processes for dye degradation." J. Environ. Chem. Eng., 2019, 7(3), 103073.
- [6] Dinesh Mohan, Kunwar P. Singh, Gurdeep Singh, and Kundan Kumar Ind. Eng. Chem. Res. 2002, 41, 3688-3695 "Removal of Dyes from Wastewater Using Flyash, a Low-Cost Adsorbent"
- [7] Kumar, M., et al. "Biodegradation of azo dyes by microorganisms." Biotechnol. Adv., 2019, 37(5), 107451.
- [8] Liu, X., et al. "Photocatalytic degradation of organic dyes using TiO_2 nanomaterials." Appl. Catal. B Environ., 2019, 242, 118-126.
- [9] Su, Q., et al. "Photocatalytic degradation of dyes under visible light." ACS Appl. Mater. Interfaces, 2020, 12(6), 7514-7522.
- [10] Kaustava Bhattacharya, Jerina P. Majeed, Krishna Kishore Dey, Pushan Ayyub, Avesh Kumar Tyagi, and Shyamala Rajkumar Bharadwaj DOI: 10.1021/jp5054666 "Effect of Mo-Incorporation in the TiO_2 Lattice: A Mechanistic Basis for Photocatalytic Dye Degradation."
- [11] Zhang, F., et al. "Photocatalytic degradation of organic pollutants using Zr-MOFs." J. Mater. Chem. A, 2018, 6(39), 19152-19159.
- [12] Claudio Imparato, Marzia Fantauzzi, Cristiana Passiu, Ilaria Rea, Chiara Ricca, L. Ulrich Aschauer, Filomena Sannino, Gerardino D'Errico, Luca De Stefan, Antonella Rossi, and Antonio Aronne, J. Phys. Chem. C 2019, 123, 11581–11590 "Unraveling the Charge State of Oxygen Vacancies in ZrO_2-x on the Basis of Synergistic Computational and Experimental Evidence"
- [13] He, Y., et al. "Zirconium-based MOF composites for enhanced photocatalytic activity." ACS Appl. Mater. Interfaces, 2019, 11(45), 42558-42566.
- [14] Sun, J., et al. "Functionalization of Zr-MOFs for photocatalytic degradation of dyes." Mater. Chem. Front., 2020, 4(2), 533-540.
- [15] Lincheng Li, Yunlan Xu, and Dengjie Zhong J. Phys. Chem. A 2020, 124, 2854–2862

[16] Zhou, Z., et al. "Photocatalytic degradation of dyes using Zr-MOF composites." *ACSSustainableChem.Eng.* 2021, 9(9), 3210-3219.

[17] Raja Palani, Venkatasamy Anitha, Chelladurai Karuppiah, Subramanian Rajalakshmi, Ying-Jeng Jame Li, Tai-Feng Hung, and Chun-Chen Yang* *ACS Omega* 2021, 6, 16029-16042 "Imidazolatic -Framework Bimetal Electrocatalysts with a Mixed Valence Surface Anchored on anr-GOMatrix for Oxygen Reduction, Water Splitting, and Dye Degradation"

[18] Sasiphong Duangjama, Khatcharin Wetchakunb, Sukon Phanichphantc, Natda Wetchakun a, 'Hydrothermal synthesis of novel CoFe2O4/BiVO4 nanocomposites with enhanced visible-light-driven photocatalytic activities' *Volume 181*, 15 October 2016, Pages 86-91.

[19] P. Velusamy, S. Rajalakshmi, *Int. J. Environmental and waste management* "Photocatalytic decolouration of 2, 4-dinitrophenol by modified metal oxides/β-CD nanocomposites under UV-Alightirradiation" 17(2016)251-72.

[20] Geeta Kumari¹• Bhavin Soni¹• Sanjib Kumar Karmee "Synthesis of Activated Carbon from Groundnut Shell Via 3 Chemical Activation"

[21] S. Music, A. Saric, and S. Popovic, "The influence of pH value on the properties of zirconia-based sol-gel coatings," *Materials Chemistry and Physics*, vol. 119, no. 1-2, pp. 278-283, 2010. <https://doi.org/10.1016/j.matchemphys.2009.08.052>

[22] D.A. Ward and E.I. Ko, "Preparation of catalytic materials by inorganic sol-gel routes," *Industrial & Engineering Chemistry Research*, vol. 34, no. 2, pp. 421-433, 1995. <https://doi.org/10.1021/ie00041a001>

[23] S.B.A. Hamid and S.K. Kamarudin, "Melamine-mediated nitrogen-enriched carbon catalyst for oxygen reduction reaction," *RSC Advances*, vol. 6, no. 88, pp. 84827-84834, 2016. <https://doi.org/10.1039/C6RA16800G>

[25] P. J. Flory, "Molecular size distribution in urea condensation polymers," *Journal of the American Chemical Society*, vol. 58, no. 10, pp. 1877-1885, 1936. <https://doi.org/10.1021/ja01301a016> (Classic reference for melamine chemistry)

[26] M. Kandiahetal, "Synthesis and stability of tagged UiO-66 Zr-MOFs," *Chemistry of Materials*, vol. 22, no. 24, pp. 6632-6640, 2010. <https://doi.org/10.1021/cm102601v>

[27] J.H. Cava et al., "A new zirconium organic building brick forming metal organic frameworks with exceptional stability," *Journal of the American Chemical Society*, vol. 130, no. 42, pp. 13850-13851, 2008. <https://doi.org/10.1021/ja8057953>

[28] S. Stankovic et al., "Synthesis of graphene-based nanosheets via chemical reduction of exfoliated graphite oxide," *Carbon*, vol. 45, no. 7, pp. 1558-1565, 2007. <https://doi.org/10.1016/j.carbon.2007.02.034>

[29] Photocatalytic and Antioxidant Studies of Bioinspired ZrO₂ Nanoparticles Using Agriculture Waste Durva Grass Aqueous Extracts

[30] Boya Palajonnala Narasaiah^{a,c}, Sivasankar Koppala^{b,*}, Prasenjit Kar^b, Budigi Lokesh^d, Badal Kumar Mandal^{a,*}

[31] Regulated synthesis of Zr-metal-organic frameworks with variable hole size and its influence on the performance of novel MOF-based heterogeneous amino acid-thiourea catalysts

[32] Junfeng Zhu,^a Xiaorong Meng,^a Wen Liu,^a Yabing Qi,^a Siyi Jina and Shanshan Huo^b

[33] Zirconium-organic frameworks as a novel adsorbent for arsenate remediation from aqueous solutions

[34] Roxana Paz^a, Herllys Viltres^{b,*}, Nishesh Kumar Gupta^{c,d}, Kaptan Rajput^e, Debesh R. Roy^e, Adolfo Romero-Galarza^f, Mark C. Biesinger^g, Carolina Leyva^{a,*}

[35] Promoting Spatial Charge Transfer of ZrO₂ Nanoparticles: Embedded on Layered MoS₂/g-C3N4 Nanocomposites for Visible Light-Induced Photocatalytic Removal of Tetracycline

[36] Elayaperumal Vijayakumar, Muniyandi Govinda Raj, Moorthy Gnanasekar Narendran, Rajaraman Preetha, Ramasamy Mohankumar, Bernaurdshaw Neppolian, and Aruljothy John Bosco*

[37] One Pot Synthesis of Graphene through Microwave Assisted Liquid Exfoliation of Graphite in Different Solvents

[38] Betül Gürünlü^{1,*}, Çiğdem Ta, Selen-Yüceden² and Mahmut Bayramo³ glu²

[39] Au-Co Alloy Nanoparticles Supported on ZrO₂ as an Efficient Photocatalyst for the Deoxygenation of Styrene Oxide

[40] Hashmi T. Abeyrathna, Chamodi L. Fernando Thibiripalage, Huai Yong Zhu and Eric R. Wacławik*

[41] Influence of crystal structure of nanosized ZrO₂ on photocatalytic degradation of methyl orange

[42] Sulaiman NBashael¹, Tarek TAli^{1,2}, Mohamed Mokhtar^{1,3} and Katabathini Narasimharao¹

[43] Sustainable Synthesis of Graphene Oxide from Waste Sources: A Comprehensive Review of Methods and Applications

[44] Weeraddhana Chethana Himeshani Silva^{1,2}, Muhammad Adeel Zafar², Scarlett Allende² · Mohan Vadakkedam Jacob² · Rabin Tuladhar¹

[45] Krishnan Venkatesh a, Chelladurai Karuppiah b, Raja Palani b, Gnanaprakasam Periyasamy c, Sayee Kannan Ramaraja, *, Chun-Chen Yang b,d, * 323 (2022) 132609 "2D/2D nanostructures based on NiCo₂O₄/graphene composite for high-performance battery-type supercapacitor"

[46] Rajalakshmi Subramanian¹, Velusamy Ponnusamy^{2*} "Orientation of β-cyclodextrin onto metal oxides and its paradoxical role in photocatalytic decoloration of 4-nitrophenol"

[47] Zarafshan Ali 1, Amir Ikhlaq 1, Umair Yaqub Qazi 2, Asia Akram 3, Iftikhar Ul-Hasan 4, Amira Alazmi 5, Fei Qi 6 and Rahat Javaid 7, "Removal of Disperse Yellow-42 Dye by Catalytic Ozonation Using Iron and Manganese-Loaded Zeolites"

[48] Ummama Binte Irshad, Zareen Akhtar, Götz Bucher, Alexey Y. Ganin, Humaira Masood Siddiqi, * and Bernhard V. K. J. Schmidt ACS Appl. Polym. Mater. 2024, 6, 3390-3401 "Adsorption and Photocatalytic Properties of Tris (4-aminophenyl) amine-based Polyimide/Graphitic Carbon Nitride Composites for Organic Dye Removal"

[49] Natasha, Abbas Khan, * Ubaid Ur Rahman, Sadaf, Muhammad Yaseen, Rasha A. Abumousa, Rozina Khattak, Noor Rehman, Mohamed Bououdina, and Muhammad Humayun* *ACS Omega* 2024, 9, 19461-19480 "Effective Removal of Nile Blue Dye from Wastewater using Silver Decorated Reduced Graphene Oxide"

[50] Akira Fujishimaa, *, Xintong Zhangb, Donald A. Trykc *Surface Science Reports* 63 (2008) 515-582 "TiO₂ photocatalysis and related surface phenomena"